Available online at www.jourcc.com

Journal homepage: www.JOURCC.com

Journal of Composites and Compounds

State of the art review of photocatalytic water treatment

Ahmed Abdelaal [a], *Farzin Banei* [b], *Angelo Fenti* [c]*, *Maryam Nili-Ahmadabbdi* [d], *Miguel Martín-Sómer* [e], *Vahid Keshavarz* [f]

[a] *Environmental Sciences Department, Faculty of Science, Port Said University, 42522 Egypt*
[b] *Department of Neurology, Shahid Beheshti University of Medical Sciences, Tehran, Iran*
[c] *Department of Engineering, University of Campania "Luigi Vanvitelli", Aversa, Italy*
[d] *Materials Engineering Department, Tarbiat Modares University, Tehran, Iran*
[e] *Department of Chemical and Environmental Technology, Universidad Rey Juan Carlos, C/Tulipán s/n, 28933 Móstoles, Madrid*
[f] *Department of Materials Engineering, Imam Khomeini International University, Qazvin, Iran*

ABSTRACT

Supplying clean water is a major problem in contemporary societies. The rise of industrialization, urbanization, and population increases have caused a shortage of clean water supplies, and the disparity between healthy water demand and availability is expected to worsen. The use of emergent organic contaminants (EOCs) and inorganic pollutants constitute a significant threat to the environment and human health.The most promising approach for water treatment is the usage of primary photocatalytic oxidation processes. The paper begins by outlining the issue of scarce water supplies and the many methods of purification, including photocatalysis using semiconductors like metal oxides, graphene oxides, and MOFs. The article also reviews published research on the application of these photocatalysts materials for the reduction of pollutants from water. This review article provides an overview of technique for photocatalytic water treatment, discussing the basic mechanism of photocatalysis and nanobased photocatalysts utilized for the reduction of organic pollutants in water.

Peer review under responsibility of UGPH.

ARTICLE INFORMATION

Article history:
Received 19 December 2022
Received in revised form 11 February 2023
Accepted 23 March 2023

Keywords:
Photocatalysis
Water Treatment
Metal Oxides
Metal organic frameworks
Carbon Materials
Nanocellulose

Table of contents

1. Introduction

Water contamination is one of the environmental issues that poses a severe threat to human health [1]. Due to the sharp development in industry, urbanization, and population, as well as a serious lack of clean water supplies, these issues have received a great deal of attention globally. It is predicted that the gap between healthy water need and availability will continue to widen in proportion to enhancing contamination because of the vast disposal of pollutants and toxins into the natural water resource. [2].

Hence, reducing and treating water pollution is very important and

* *Corresponding author: Angelo Fenti; E-mail: angelo.fenti@unicampania.it*

https://doi.org/10.61186/jcc.5.1.7

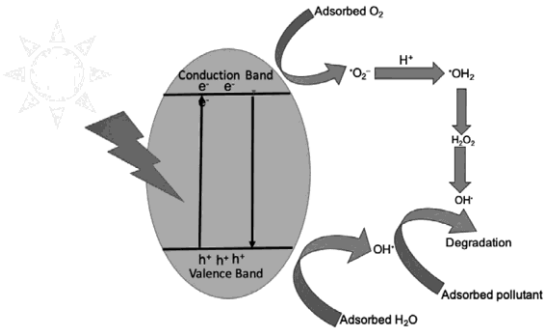

Fig. 1. Mechanistic view showing photocatalysis and degradation of pollutant

essential. Many sources with a variety of intricate components lead to water pollution. Many emergent organic contaminants (EOCs), such as pharmaceuticals, personal care items, industrial pollutants, and others, have been identified in recent years as polluting water resources [3, 4]. The majority of EOCs, even at low concentrations, are difficult to entirely remove by conventional water treatment techniques because of their physical or chemical characteristics (such as high-grade and water-soluble) [5].

Together with EOCs, inorganic pollutants constitute a significant hazard to both the health and the environment because of their toxicity, carcinogenicity, mutagenicity, and teratogenicity. Hence, a variety of methods and procedures, including coagulation, filtration, and other methods, have been suggested to cleanse wastewater [6, 7]. These approaches are not ideal, though, as they require elaborate, sizable facilities that cost a lot to maintain [8].

The methods that rely on principal photocatalytic oxidation processes are the most promising for treating water. This is because wastewater is becoming more complex, particularly because of the tenacious biological, poisonous, and organic chemicals.

Water treatment using photocatalytic methods is a relatively new field with exciting potential that will be put into practice soon [9]. The photocatalytic oxidative destruction of man-made and naturally occurring organic contaminants (such as pesticides, organic fertilizers, humic matter, surfactants, etc.) in the photic layer covering surface waters is of highest importance among the many physicochemical changes occurring in the hydrosphere. Due to the intensity of the UV component of solar energy reaching the Earth's surface, which is brought on by the expansion of ozone holes in the stratosphere, environmental photochemical processes are becoming increasingly important [10].

This review article offers an overview of the knowledge and advancement of photocatalytic water treatment technology, covering everything from the principles of catalyst and photoreactor creation to process optimisation and the water conditions that influence the procedure's effectiveness.It also discusses the basic mechanism of photocatalysis and nanobased photocatalysts used for the reduction of organic water and wastewater contaminants This multidisciplinary article provides chemists, materials scientists, and engineers working with water with a revised and insightful analysis of recent findings on nanomaterials photocatalytic degradation-focused research in contrast to reviews that have already been published. The paper examines various chemical modification techniques for improving the nanomaterials surface chemistry in order to remove specific contaminants like organic colors and drugs from water efficiently.

2. Photocatalytic water treatment

Photocatalysis has been recognised as one of the most exciting possibilities for water treatment to date because of its enormous capacity and effectiveness in using sunlight to destroy harmful bacteria and organic

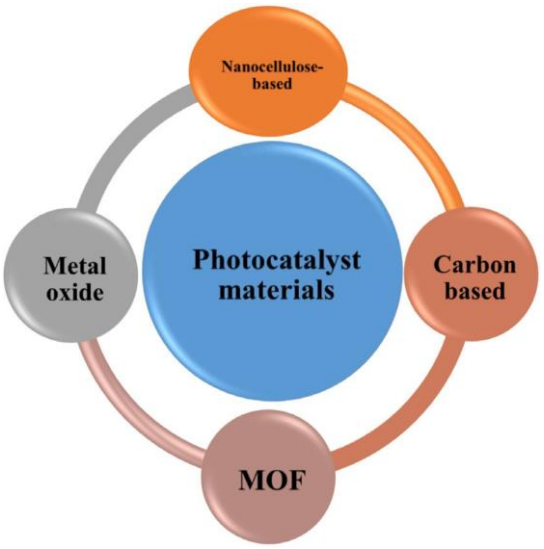

Fig. 2. Materials toward photocatalytic application.

contaminants.[11, 12]. It is common knowledge that the nature of the used photocatalysts has an impact on the photocatalytic efficiency, but that the irradiated light source also has an impact. Typically, a photon that has energy equal to or higher than its band-gap energy (Eg) can photoactivate the catalyst. Normally, the photolysis reactions would be more efficient with a higher irradiation intensity. [13]. Natural sunlights is the best resource to provide energy for these activation procedures because it is secure and renewable. Also, solar energy has unique benefits including its abundance and cleanliness. The energy that the sun provides to the surface of the earth each year is roughly four orders of magnitude greater than the energy that people utilize worldwide each year [14]. It has a lot of allure to investigate innovative catalysts having photocatalytic activity triggered by visible light to more effectively use solar energy to address water pollution challenges [15].

Photocatalysis is an intriguing advanced oxidation process used for breaking down organic pollutants and deactivating harmful biological agents. Heterogeneous photocatalysis is particularly useful in water treatment due to its advantageous characteristics, such as operating at feasible temperatures and pressures, completely decomposing pollutants and their intermediate products without producing any more contaminants, and being economically reliable. By creating reactive oxygen species (ROS) such as holes (h^+), $\bullet O_2$-, H_2O_2, O_2, and •OH, photocatalysis can facilitate the breakdown of pollutants through reactions with dissolved O_2 or H_2O/OH-. Moreover, optimal energy conversions can be achieved by reducing H^+ or CO_2 to H_2 or hydrocarbons while converting H_2O/OH^- to O_2 through oxidation. The high oxidative power of ROS and holes facilitates the effective breakdown of pollutants and increases the rate of the reaction [16]. The production of the superoxide radical occurs when photogenerated electrons of a semiconductor's conduction band (CB) react with O_2, while the production of the • is a result of the reaction between valence band holes (h^+) . This can be expressed through equations 1 and 2 [17].

$$e^-_{CB} + O_2 \rightarrow \square O_2^- \quad (1)$$

$$h^+_{VB} + H_2O \rightarrow \square OH + H^+ \quad (2)$$

3. Photocatalytic mechanism

According to the energy band hypothesis, at absolute zero, a semiconductor's valance band (VB) contains electrons with a lower energy whereas CB is unoccupied and has a correspondingly higher energy., can be used to explain photocatalysis. When a semiconductor absorbs visi-

ble light, its VB electrons are move to higher CB levels, causing holes to remain. As a result, the semiconductor's VB becomes occupied with holes, while its CB fills up with electron accumulation. Following their migration to the semiconductor material's surface, these photogenerated charge carriers next take part in redox processes. Due to their reductive character, photogenerated electrons contribute to the production of ROS, which enhances the efficiency of photocatalysis, while photogenerated holes have high oxidative properties [18, 19].

It is important to note that not all photo excited electrons contribute to surface reactions that generate active species. A number of electron combine with the semiconductor' VB holes, leading to a reduced photocatalytic efficiency. Therefore, the critical process in improving photocatalytic effectiveness is to prevent the recombination of charge carriers produced by lighten promote their movement to the semiconductor's surface, that they can react with water and O_2 to generate •OH and •O2-, respectively. This reaction inhibits electron-hole pair recombination and extends their lifespan. The pace of movement and recombination of photocarrier is influenced by the potential of the VB and CB edges and the redox properties of the adsorbates.

In order for redox reactions to occur, the VB potential must be more positive and the CB potential must be lower than the equivalent redox abilities necessary for the reactions of the surface. [20, 21]. However, it is hard for a single-component photocatalytic system to meet all certain essential criteria. In contrast to a semiconductor system with a wide band gap, which makes it hard to produce electron-hole pairs (EHP), one with a narrow band gap undergoes rapid photocarrier recombination. To increase the photocatalytic efficacy of semiconductor photocatalysts, various strategies are employed. These include surface functionalization through the addition of co-catalysts and the utilization of the plasmonic impact, surface modulation through the creation of defects via elemental and molecular doping, and the preparation of surface assemblies via the conventional fabrication and systems of Z-scheme heterojunction [22, 23].

Among the strategies mentioned above, the creation of a heterojunction by adding some semiconductor materials with appropriate band-edge potentials has received significant attention because of several reasons. Firstly, it allows for the improvement of visible light harnessing by coupling a photocatalyst with a broad band gap with another semiconductor material that has a narrow band gap. Secondly, it stimulates the separation and migration of photocarriers through induced internal electric fields. Lastly, it allows for the preservation of EHP provide high redox and oxidative ability, respectively, in various semiconductor photocatalysts, leading to enhanced redox ability [23, 24]. Generally, an active species that facilitates pollutant breakdown and a light-harvesting antenna compose up the heterogeneous photocatalysis system employing semiconductor materials. There have been numerous proposals for the sequence of redox reactions that take place at the photon-activated surface. [17]:

$$Photocatalyst + hv \rightarrow h^+ + e^- \quad (3)$$

$$h^+ + H_2O \rightarrow \bullet OH + H^+ \quad (4)$$

$$h^+ + OH^- \rightarrow \bullet OH \quad (5)$$

$$h^+ + pollutant \rightarrow (pollutant)^+ \quad (6)$$

$$e^- + O_2 \rightarrow \bullet O_2 \quad (7)$$

$$\bullet O_2^- + H^+ \rightarrow \bullet OOH \quad (8)$$

$$2 \bullet OOH \rightarrow O_2 + H_2O_2 \quad (9)$$

$$H_2O_2 + \bullet O_2^- \rightarrow \bullet OH + OH^- + O2 \quad (10)$$

$$H_2O_2 + hv \rightarrow 2 \bullet OH \quad (11)$$

Table 1.
Metal oxide, MOF materials, C-Based materials and NC-Based materials for watertreatment application

	Materials	Target	Light Source	Degradation Rate	Ref.
Metal oxide	TiO_2/Ag ZnO/Ag NiO/Ag	methyl orange(MO)/4-chlorophenol	Visible light	86%-180 min for MO 68%-180min for 4CP	[161]
	CTAB-assisted TiO_2	Congo red dye	Sunlight	95%- 180 min	[162]
	Fe_2O_3@C@SiO_2/TiO_2	organic dyes	Visible light	97%	[163]
	Fe-TiO_2	organic dyes	Sunlight	85%-210min	[164]
MOF materials	MIL-125 F-MIL-125 TiO_2@MIL-125 F-TiO_2@MIL-125	PFOA	Visible light		[165]
	CoCeOx/g-C3N4	carbamazepine	Visible light	97%-60 min	[166]
	PCN-224/TA/PVDF	organic dyes	Visible light	98%-60 min	[167]
	Ag NPs@Zr-TTFTB	sulfamethoxazole	Sunlight	99%-120 min	[168]
	UiO-66-NH_2	sulfamethoxazole	Sunlight	90%	[169]
C-Based materials	porous carbon nitride nanosheet (MCU-C_3N_4)	tetracycline hydrochloride (TC)	visible light	84.81%	[170]
	Sand-graphite	methylene blue(MB)	visible light	87.12 %	[171]
	carbon quantum dots (CQDs) functioned polymer carbon nitride (PCN)	Bisphenol A	visible light	95%-30min	[172]
NC-based Materials	Ag_3PO_4/nanocellulose	MO/ MB	Sunlight	90%-80min	[173]
	Fe-doped ZnO/nanocellulose	MB	visible light	98.84%	[174]
	Anatase TiO_2/nanocellulose	MO	visible light	99.72%-30 min	[175]
	ZnO/NC	Enrofloxacin (EF)	visible light	97%-120 min	[176]
	NC–TiO_2	MO	visible light	99%-180 min	[177]

Pollutant + $(\bullet OH, h^+, \bullet OOHor O_2^-)$ >degradation product (12)

Photocatalytic reactions typically involve three active species: h+, hydroxyl radical (•OH), and superoxide radical ($\bullet O^{2-}$), with •OH being the primary oxidant in aqueous solutions. •OH radicals are produced through two pathes: (i) photogenerated h+ oxidizes H_2O and OH- in the water to form •OH radicals, and (ii) photogenerated e- reduces $\bullet O^{2-}$ to create $\bullet O_2$ radicals, that react with h^+ to form •OOH radicals and further decompose to generate •OH radicals. Photogenerated h+ can directly degrade organic contaminants, but its efficiency lies on the oxidation conditions and catalyst type. However, e- and h^+ can easily recombine in the hole scavengers or absence of electron. Thus, the existence of specific scavengers is essential to suppress charge recombination rates and improve photocatalytic efficiency [25]. The fundamental process of semiconductor photocatalysis depicted in Figure 1.

Building a reliable and effective photocatalytic device that responds to visible light requires consideration of not only electronic band structures but also other parameters like material choice, morphological architecture, surface properties, and crystallinity. The selection of semiconductor materials is crucial in determining the level of overall efficiency and visible light response. Effective carrier separation and transportation can be achieved with the appropriate morphological architecture, which involves a short distance between the redox reaction center and photo carrier-generating junction. Low interface recombination and high crystallinity with structural defects can improve the ability of photogenerated holes and electrons to participate more effectively in desired processes. The photocatalysts' surface area, that is determined by the shape of materials' geometrical and porosity, also plays a critical role in photocatalytic activity because of the importance of pollutant adsorption.

4. New materials toward photocatalytic application

4.1. Metal oxide

In recent times, TiO_2 and ZnO nanoparticles (NPs) have gained great attention as semiconductor photocatalysts, because of their high catalytic efficiency, high chemical stability, bio-compatibility, low cost, and ease of synthesis [26]. Both TiO_2 and ZnO possess excellent properties that make them nearly ideal photocatalysts, as they respond to radiation intensity equal to or below UV wavelength. On the other hand, zinc oxide is more sensitive to photo-corrosion rather than TiO_2, despite being more stable, providing smaller defects, and crystallinity.[27]. Moreover, the performance of photocatalytic activity of ZnO can be further enhanced by doping or adding other materials. Recently, metal oxides, like Fe_2O_3, WO_3, TiO_2, ZrO_2, ZnO, V_2O_5, etc., have been utilized as photocatalysts to eliminate or reduce harmful inorganic and organic constituents in air or water resources. These photocatalysts offer a great deal of potential for converting different pollutants into biodegradable constituents, ultimately transforming them into safe CO2 and water. [28, 29]. TiO_2 was synthesized by Tayade and coworkers [30] using the hydrolysis approach, and transition metals (Ni, Cu, Ag, Fe, and Co) were subsequently doped onto titanium oxide using the wet impregnation technique. Acetophenone and nitrobenzene in aqueous solution were photo-degraded using these samples, and the Ag-doped catalysts had the best activity. When MB and MG were subjected to UV irradiation for 60 minutes, the photocatalytic efficiency of synthetic titanium oxide When MB and MG were tested for degradation by NPs, it was found that nearly 71% and 78% of MB and MG, respectively, were decolored due to the presence of TiO2 NPs. The effectiveness of photocatalytic degradation with or without a photocatalyst as well as the impact of a light source were compared by Harun et al. [31]. Congo red dye was decolored using titanium oxide as a photocatalyst in solar and artificial UV light, and when compared to artificial UV radiation, it was found that sunshine may destroy the dye up to 66.99% in 30 minutes. In 2016, MB, Acridine orange (AO), and RhB, were among the dyes that were degraded photocatalytically using ZnO and TiO_2 NPs, according to a report by Amini and colleagues [32]. This was done at ambient temperature and solar light irradiation. They discovered that when ZnO was swapped out for TiO2, the system's photocatalytic activity was significantly boosted as a result of the instability and consequent deactivation of ZnO particles. The activity of 1D nanostructures zinc oxide and titanium oxide (nanotubes and nanorods) for removing of MO dye was also contrasted by Guo et al. [33]. The results showed both of them had similar photocatalytic efficiency, with ZnO being more effective when exposed to sunlight and TiO2 being more effective when exposed to UV light.

Cu-ZnO was employed by Kanade et al. [34] to produce photocatalytic hydrogen, and it was tested under visible light irradiation after being synthesized in both aqueous and organic mediums. Cu-ZnO produced in organic media has a greater photocatalytic activity than Cu-ZnO produced in aqueous media. The prismatic form of wurtzite ZnO has ZnO as part of its structure and Cu as oxide in the core. Mn-doped ZnO NPs were used in photo-degradation by Ruh Ullah et al. [35]. Aniline and MB dyes were degraded using visible light from a tungsten bulb to gauge the photocatalytic effectiveness of Mn-doped ZnO NPs. Results demonstrated that Mn-doped ZnO degraded 50% more fast than undoped ZnO, indicating that ZnO:Mn^{2+} NPs are more effective for disinfecting water from inorganic and organic compounds, such as bacteria and arsenic . Using undoped ZnO:Mn2 and ZnO + under UV light irradiation, the first photo-reduction of MB was carried out. Although ZnO:Mn2+ took 30 minutes to destroy the same amount of MB, undoped ZnO was more effective than doped ZnO. Undoped ZnO degraded over 50% of MB in 10 minutes. Donkova et al. [30] conducted a study utilizing undoped Mn or Cu doped ZnO as photocatalysts that were prepared through chemical methods. Under UV light irradiation, their photocatalytic efficiency for MB the removing of dye was examined. Pure ZnO was able to degrade the dye completely in 2 hours, while the catalysts with the maximum additive of Mn and Cu only achieved 30% degradation in 2 hours. The study found that photocatalytic activity decreased as doping increased for all the samples examined. More recent studies have shown that several materials such as nanocomposites NiO/ZnO, PVDF/GO/ZnO, TiO_2/Fe_3O_4/graphene oxide and WO_3/TiO_2, as well as ZnO/Ag heteronano structures and N_2 doped TiO_2 thin film, are effective in the photo-degradation of MB in visible-light irradiation [31-34].

Labhane and coworkers [35] synthesized Cu-doped ZnO nanoparticles with varying percentages of Cu (0%, 1%, 2%, and 3%) using the co-precipitation method. The optical absorption spectroscopy of Cu-ZnO revealed a decline in band gap with an enhancement in Cu content. The catalytic performance of the synthesized samples was examined by degrading MB under UV light illumination, and undoped ZnO exhibited higher performance than Cu-doped ZnO. In another study by Min Fu et al. [36], Cu-doped ZnO NPs were prepared using the sol-gel procedure, and their photocatalytic performance was examined by degrading MO. The highest degradation rate achieved was 88% within 3 hours, that was higher than that of undoped ZnO. Upon surveying various articles, it was found that the primary issue with TiO_2 NPs was its recombination of EHP was very fast, leading to a reduction in photocatalytic efficiency. To address this problem, the addition of metal oxides and metals into the TiO_2 matrix considered as an effective solution. For example, a Ce-TiO_2 nanocomposite was synthesized and utilized as a photocatalyst for the removing of sodium diclofenac, acid red (AR), and rose Bengal (RB), with different factors, like time of irradiation, photocatalyst amount, and pollutant concentration, being evaluated [37]. Similarly, Nasir et al. investigated the photocatalytic performance of TiO_2 NPs filled with noble

metals (M-TiO_2, where M = Pt, Ag , and Au) for the effective reduction of acetaminophen (AP) under solar light [38]. The photocatalytic degradation of AP was investigated with various factors like photocatalyst dose, initial pH, initial AP concentration, surfactants, noble metal loading, and solar light intensity. The results revealed that the performance of M-TiO_2 photocatalyst was superior compared to conventional TiO_2 NPs. In other words, the incorporation of noble metals not only scavenged electrons that produced from TiO_2 NPs, caused to an increase in electron/hole separation, but also enhanced the capacity of M-TiO_2 to adsorb solar light. Furthermore, the incorporated noble metals played a vital role in the generation of reactive species like H_2O_2, •OH, •O_2-, and •OOH, and that directly affected the activity of TiO_2 NPs photocatalyst. Pt-TiO_2 exhibited better photocatalytic efficiency among them. In another study, the photocatalytic degradation of sulfamethoxazole was experimented using single (Au, Cu, and Ag) and bi-metallic (Au-Cu and Au-Ag) deposited on TiO_2 NPs under sunlight and UV irradiation [39]. As previously stated, the addition of metal oxides like WO_3, Al_2O_3,ZrO_2 and $SiO_2$to TiO_2 NPs can enhance their photocatalytic properties. Hir and coworkers, fabricated photocatalysts film of polyethersulfone-TiO_2 with different amounts of TiO_2 NPs [40]. The photocatalytic performance of polyethersulfone-TiO_2 was tested using methyl orange (MO) as a model dye. Results indicated that 13 wt% of TiO_2 NPs could remove all of MO. In order to remove multi-drug resistant Escherichia coli (MDR E. coli), Das et al. [41] prepared Fe/ZnO NPs as a photocatalyst using the chemical precipitation technique. The photocatalytic reaction was performed for 90 minutes in solar light.It was observed that Fe/ZnONPs removed over 99.9% of MDR E. coli, exhibiting superior performance compared to pure TiO_2 and ZnO. However, since the band gap of TiO2 and ZnO is wide, they cannot efficiently absorb visible light, resulting in limited utilization of solar radiations. To address this issue, several approaches have been investigated, such as deposition of noble metals, coupling of different semiconductor systems among others, and doping of transition metals[42]. The findings indicate that coupling different semiconductor oxides leads to a reduction in band gaps and an extension of the absorption range to the visible light region. This promotes the separation of electron-hole pairs, resulting in an increase in photocatalytic performance [43]. Among the available metal oxides, ZnO is a good photocatalyst because of its ease of fabrication, low cost, excellent oxidation capacity, and large free excitation binding energy. Additionally, within TiO2 NPs, photo-generated electron-hole pairs recombine quickly. Thus, several strategies have been explored to facilitate of TiO_2 photocatalyst in visible-light, including adding different materials to enhance its photocatalytic performance [44]. One study employed glucose to synthesize carbon-doped TiO_2 photocatalyst for RhB photo-reduction [45]. This approach led to the substitution of carbon elements in the TiO_2 structure, resulting in a mesoporous material with a bandgap of 3.01 eV, a micropore diameter of 8 nm, and a surface area of 126.5 m^2/g. The photocatalytic degradation of RhB was studied by varying factors like irradiation time, substrate amount, and TiO_2/RhB ratio. ZnO faces limitations as a photo electrode due to its n-type behavior, which impedes its control of electrical conductivity [28]. However, doping ZnO with transition metals such as Al, Fe, Ag, Cr, Mn, and Co can modify its electrical, optical, and magnetic properties based on doping concentration [46]. Active sites are created by surface defects, thus, studying the effect of doped ZnO on photocatalytic performance is crucial [47].

4.2. MOFs material

MOF materials are typically prepared by combining organic ligands and metal-containing units through coordination, resulting in an open network structure with remarkable features such as high porosity, stability, pore size, and enormous surface area[48]. Organic linkers such as neutral organic molecules, halides, cyanides, and anionic organic molecules [49]. The geometry of the resulting MOF structure is determined by metal's coordination number at the center and can range from linear to T- and Y-shaped structures [50]. Both the organic and inorganic components can form structures with high flexibility and n-dimensional (n = 1, 2, 3) complexity, allowing for combination with guest molecules. MOFs consist of weaker bonds than zeolites (such as H2 bonds and coordination) between organic-inorganic bonds, that contribute to the MOF's structural stability under various hard conditions [51]. MOFs have had a long-lasting impact on various fields including chemistry, material sciences, and physics, biology. Initially, MOF nanomaterials were prepared by combining organic linkers and metal cluster ions with strong bonds to form a permanent, open porous crystalline network [52]. These materials possess a range of advantageous characteristics like high porosity, stability, large surface area under different environments, and an inexpensive preparation process. [53]. The ligands play a critical effect in forming symmetric pore distribution, which result in increased adsorption ability. The enormous dimensions of MOF pores often result in a large pore size (over 10 Å in numerous MOF framework), while others have a narrower pore size distribution, leading to a relatively stronger adsorbent-adsorbate bond [54]. The use of metallic ions with different organic linkers has allowed researchers to develop an extensive variety of MOF materials [52].

Two critical features in selecting the appropriate MOF for wastewater treatment are the pore environment, that can be modified by altering the surface area and the organic ligands. MOF have been identified as potential alternatives because of their homogeneous distribution of topological structure, active sites, and inherent properties of organic-inorganic hybrids. MOFs exhibit attractive semiconductor properties, enabling the integration of various molecular functional components to activate incident light and promote diverse useful photocatalytically reactions [55].. Photo-reducation occurs when there is a distinction in energy between the illuminated light and the band gap energy. MOF is regarded as a photocatalyst because, when exposed to light, it behaves like a semiconductor. [56].. Some experiments have been conducted which using MOF for photocatalysis, yielding satisfactory outcomes that make them appropriate.

Zhang et al. presented a unique system in 2015 for the removal of brilliant green (BG) and fuchsine acid (AF) under visible light that consists of Pd NPs supported on MIL-101(Cr) with reduced graphene oxide (rGO) . This photocatalystwas cyclable for five cycles and had a photocatalytic capacity of 100% for BG in only 15 minutes (20 minutes for AF). [58]. The hierarchical MIL-100(Fe)33% @TiO2 revealed 45 times the highest rate of MB in comparison with TiO_2 because the MOF-based photocatalyst's superior adsorption ability, which has a larger surface area than TiO2, provided suitable reaction channels and made it easier to capture the organic dye. A further illustration is the MOF-based heterogeneous structures made of MIL-53(Fe) microrods ornamented with magnetic nanospheres, which shown remarkable efficacy in the H2O2-mediated visible light RhB photo breakdown technique and reached up to 98.7% RhB degradation. [55]. Additionally, RhB was completely destroyed by MIL-53(Fe)@AgI after 180 minutes of visible light exposure [60]. Some MOFs, including MOF-5 and UiO-66, can act as semiconductors, transferring energy from the organic linker to the metal-oxo cluster. [61]. The usage of solar energy is constrained by the fact that the majority of MOFs can only harvest UV light. MOFs have been coupled with sensitizers and semiconductors to overcome this restriction. For instance, the photoreduction of sulphorhodamine B was greatly increased by the composite system of MIL-53(Fe) and the cationic resin Amberlite, and the degradation was effective for five cycles [62].There are various strategies reported in literature for the development of photoactive materials based on MOFs, which are grouped into three categorized based on their photocatalytic mechanism [58, 59]. The first method utilizes the semiconductor characteristics of metal clusters,

resulting in dispersed nano semiconductors which are isolated by organic linkers, and yielding type I MOFs. These MOFs are advantageous as they possess high porosity that enables pollutants to be in close proximity to the photogenerated charges and semiconductor dots, light absorption, and photoactive dots' high density by the organic linker acting as antennae, thereby enhancing the photo response of the catalyst [58]. When creating type II MOFs, organic linkers with photo responsiveness, like dye-based linkers, are used. These linkers act as antennas, collecting light and transferring charges produced by photosynthesis to the metal clusters.. [60]. Type III MOFs are the simplest method, in that the MOFs act as a photoactive species and porous matrix are encapsulated within the porous structure. Their stability in water was a significant drawback. For instance. A study on the photo reduction of phenol in water using MOF-5 was carried out by Alvaro et al., however, its instability was later observed by Hausdorf and coworkers [62], who noted that its structural modification was influenced by the water environment. Laurier and coworkers. [63] reported the photocatalytic performance of Fe-based MOFs, such as MIL-88B, MIL-101, and MIL-100, which all contain Fe3-µ3-oxo clusters, for the reduction of Rhodamine 6G under visible light . These MOFs had higher activity than virgin TiO_2 and rather well retained their crystallinity following the process, despite the incomplete dye degradation. The type II photocatalytic MOFs MIL-125(Ti), UiO-66(Zr), and ZIF-8[64] and the type I MOFs MIL-101, MIL-88B, and MIL-53 [60, 65] are among those that have received the most attention. In type I MOFs, the Fe-O cluster makes use of the light, and the photogenerated electron is transferred from O^{2-} to Fe^{3+}. The study also presents other effective strategies for enhancing the photocatalytic activity of MOFs, with the goal of increasing their absorption of visible light and improving their performance under solar light. Shi and coworkers [64] prepared Fe-MOFs functionalized with amino groups (NH2-MIL-53, NH2-MIL-88B, and NH2-MIL-101), which demonstrated high stability and performance for the photo degradation of Cr(VI) in water in visible light. They supposed that the addition of the amino group in the organic linker improved the performance of the MOFs due to both the Fe-cluster and NH_2-linker were excited under visible light. Another strategy for designing better photocatalysts is to deposit metal NPs onto MOFs. Theophylline, bisphenol A, and ibuprofen were three PPCPs (Pharmaceuticals and Personal Care Products) that Liang and colleagues [67] recently added Pd NPs onto MIL-100(Fe), producing highly active photocatalysts for the visible light-induced photoreduction of these three PPCPs. It was discovered that Pd NPs decreased photogenerated electron-hole pair recombination, which increased activity of photocatalyst. Heterojunctions, which are created by mixing MOFs with other semiconductors, have also showed potential. More active centers can result from the other semiconductor dispersing more easily due to the porous structure of the MOF [60]. For example, Rahimi and Mosleh[65] recently studied the photodegradation of the pesticide abamectin using a combination of $Cu_2(OH)PO_4$ and HKUST-1 through sonophotocatalysis. The MOF exhibited a band gap of 2.59 eV and achieved almost complete removing of the pesticide.

4.3. Carbon based materials

Carbon nanomaterials have demonstrated considerable promise as effective antibacterial agents, including carbon nanotubes (CNTs), fullerenes, and graphene-based materials. Among these materials, graphene is a recently findly nanomaterial that has exceptional properties such as high electrical conductivity), high charge carrier mobility at room temperature[66, 67], [68], high thermal conductivity, large surface area [69], high mechanical stiffness, optical transparency [70], [71], [72], and an exceptionally conjugated structure. Due to its biocompatibility and unique characteristics, graphene is well-suited for diverse applications such as liquid crystal devices, disinfection of bacteria, sensors, wastewater treatment, solar cells, batteries, and capacitors[73-75]. One emerging area of interest is the use of graphene composites for solar light-driven bacterial disinfection, which takes advantage of graphene's ability to transport charge carriers in photocatalytic reactions. Although graphene has found numerous applications in different fields, its use in biological studies is relatively limited. As a result, recent study has focused on understanding the interactions between living cells and graphene derivatives Studies have shown that both GO and rGO exhibit strong antibacterial performance. GO exhibits stronger antibacterial activity compared to rGO because of the smaller nanosheets' size. The van der Waal interactions between rGO nanosheets are stronger, causing particle aggregation and resulting in rGO nanosheets that are around nine times larger than GO nanosheets. Graphene sheets' cutting edges damage the cell membrane, which results in a loss of the membrane's integrity, the release of cellular material, and eventually, cell death. This bactericidal effect has been observed for both GO and rGO [76-78].

Nanomaterials based on graphene have the ability to oxidize various components of bacterial cells, including lipids, DNA, and proteins. The antibacterial properties GO and rGO have been assessed to depend on both concentration and time. Enhancing the incubation concentration and time of these materials results in a higher rate of bacterial cell death. GO dispersion shows a much higher level of antibacterial activity at all tested concentrations and incubation intervals. Both their effects on the membrane and the resulting rise in oxidative stress are thought to be responsible for rGO and GO's ability to kill bacteria. It is commonly acknowledged that the primary mechanism behind the antibacterial activity of carbon-based nanomaterials like fullerene and CNTs involves oxidative stress. [79, 80]. In general, graphene-based materials are thought to undergo oxidation through two pathways: ROS and ROS-independent pathways. Similar to fullerene, which uses a graphene-based substance to oxidize a crucial cellular component, this ROS-independent method prevents respiration or disrupts a particular microbial function. Due to its capacity to combine with other nanomaterials to form composites, graphene and its derivatives have been favored for the creation of hybrid nanocomposites. By absorbing photo induced electrons from the metal's CB, graphene can successfully separate an electron-hole pair. Due to the high water solubility of chemically altered graphene, such as GO with hydroxyl and carboxyl groups, rGO-based composites can produce hybrid materials with the necessary characteristics. It has been successful to create a number of GO, graphene, and rGO-based hybrid materials using different metal oxides, metals, non-metals, etc. [81].

The effectiveness of GO sheets as an antimicrobial agent is influenced by their morphology and lateral dimension. Larger GO sheets, for example, demonstrate greater antimicrobial performance rather than smaller ones due to their ability to cover a significant portion of the cell surface. The larger GO sheets (> 0.4 m^2) have the ability to encircle the bacterial cell, blocking all active sites on the cell membrane that are available and preventing cell division. Smaller GO sheets (0.2 m^2), on the other hand, may adhere to the surface but are unable to enclose and isolate the entire cell, leading to a noticeably lower level of performance. [82].

Metal/semiconductor-based nanomaterials are currently the most widely used photocatalysts, but they can lead to secondary pollution when metal ions are released [83, 84]. To address this issue, various non-metallic nanocarbon materials (NCMs), such as graphitic carbon nitride (g-C_3N_4), graphene, carbon dots (C-dots), and CNTs, have been studied as photocatalysts or catalyst to form heterostructured photocatalysts that enhance the photocatalytic efficiency for water disinfection.

Due to its exceptional photocatalytic activity, g-C_3N_4has attracted the most attention among these materials [85, 86]. However, due to its modest surface area and quick recombination charge carriers, bulk g-C_3N_4 with stacked layers has relatively low photocatalytic antimicrobial efficiency. Exfoliated g-C_3N_4 nanosheets are one example of a nanostruc-

ture that can be created to alter the photocatalytic antibacterial efficacy of g-C_3N_4 [87, 88].

The process to produce single atomic layer g-C_3N_4. has involved thermally etching bulk g-C_3N_4 into nanosheets and then exfoliating those sheets using ultrasonication. [85]. Greater antibacterial activity, reduced charge-transfer resistance, and improved charge separation towards E. coli were all characteristics of the resulting single atomic layer, g-C_3N_4. Mesoporous g-C_3N_4 nanosheets were created in the meantime using a two-step template-free process, resulting in porous g-C_3N_4 nanosheets (PCNS) with 2.0 nm thickness, 0.61 cm^3/g^1 of pore volume, and 190.1 m^2/ g^1 of surface area. Greater antibacterial activity was observed in PCNS in comparison in bulk g-C_3N_4 due to the presence of more reactive surface sites, quicker separation of photogenerated EHP, and increased charge transfer activity. For instance, under visible-light irradiation, PCNS obtained a disinfection rate of approximately 99.9999% in 30 minutes, but bulk g-C_3N_4 could only kill 77.1% of the same pathogens [90]. Lately, Teng and coworkers demonstrated that edge-functionalized g-C_3N_4 can be used to treat water with high pathogen content, resulting in a disinfection efficiency of over 99.9999% in just 30 minutes of visible-light irradiation. several g-C_3N_4-containing nanocomposites have been created for photocatalytic water treatment. One illustration is the construction of commercial cellulose acetate (CA) membranes with g-C_3N_4/rGO composites. This composite profited from the photocatalytic effectiveness of g-C_3N_4 in visible light, the capacity of rGO to transfer electrons, and the retention capabilities of cellulose acetate membranes. The g-C_3N_4/rGO/CA membranes efficiently eliminated all bacteria after being exposed to visible light for two hours, leading to a 6.5-log reduction in bacterial cell count [91]. The immobilization of SnO_2 and g-C_3N_4 on TiO_2 nanotubes produced on Ti plates resulted in another ternary nanocomposite with strong antibacterial efficacy under UV and visible-light irradiation [92]. To control the speed and course of photo-generated EHP and boost the disinfectant action against S. aureus, Li and colleagues created a sandwich-structured g-C_3N_4/TiO_2/kaolinite [93]. Recently, Kang and coworkers, developed two rapid and eco-friendly methods for synthesizing porous g-C_3N_4, opening up the possibility for large-scale formation of g-C_3N_4 for water disinfection applications [86]. Other nanocarbon materials (NCMs) such as CNTs, C-dots, graphene, and its derivatives, in contrast to g-C3N4, are ineffective photocatalysts for direct photocatalytic water disinfection. This is mainly due to their hydrophobic surface, which makes it difficult for them to be well dispersed in aqueous solutions [87, 88]. Additionally, their small band gaps limit their ability to effectively generate EHP, causing to low creation rates of ROS and poor antibacterial activity [89]. In order to boost the photocatalytic activity of diverse NCMs, recent research has concentrated on coupling them with metal-based photocatalysts. For example, graphene and TiO2 NP nanocomposites have been carefully explored for photocatalytic water disinfection. [90]. One work showed how to photocatalytically treat GO with TiO2 NPs under UV irradiation with methanol as a hole acceptor to create a TiO_2/rGO nanocomposite. Under natural sunlight, the resultant nanocomposite demonstrated the capacity to eradicate both F. solani and E. coli. [90]. Another study by Zeng and coworkers reported the development of a TiO_2 co-decorated rGO and C-dot nanocomposite, known as CTR. CTR demonstrated improved photocatalytic performance for bacterial inactivation under solar light, causing to morphological changes in bacterial cells. Highly dispersed C-dots and TiO2 were thought to be responsible for the more efficient disinfection because they promoted the separation of electron-hole pairs, allowed electron transfers from photo-excited O2 and TiO2 molecules via conductive rGO nanosheets, and created a lot of O2•- [99]. For possible photocatalytic water disinfection applications, NCMs have been coupled with different photocatalytic metal/semiconductor NPs. For instance, WO_3 nanorods and TiO_2 nanocrystals were anchored concurrently on rGO nanosheets, while TiO_2 was also coupled with MWCNTs [91]. In one study, a TiO_2/MWCNTs/Si film was utilized as photocatalysts for the inactivation of E. coli in visible light irradiation, resulting in a 75% bacterial kill rate in 1 hour compared to 40% in the dark [92]. Various CNT concentrations were used to generate CNT-doped TiO_2 thin films, with the composite film containing 20 weight percent CNTs demonstrating the best antibacterial effectiveness against E. coli in visible light. [93]. Although other NCMs have been combined with photocatalytic metal NPs for the photocatalytic inactivation of E. coli, these studies are not discussed in detail here [94, 95].

4.4. Nanocellulose-based material

Cellulose is a commonly used biopolymer for reinforcing composites made of fiber and thermoplastic materials [96]. Nanocellulose (NC) is extracted from cellulose in nanoscale dimensions and can take various forms. It is a renewable material with a high surface area, strength, unique surface chemistry, and chemical inertness [97]. Two forms of NC are cellulose nanocrystals (CNCs) and cellulose nanofibrils (CNFs), with a rod-like shape and lengths ranging from 100 nm to 2000 nm and diameters between 2 and 20 nm [98]. The forms and sizes of NC depend on the source of cellulose and the preparation method used [99]. Acid hydrolysis is a common method used in the preparation of nanocelluloses, using either hydrochloric or sulfuric acid. During this process, the acid reacts with the hydroxyl groups on the surface of cellulose to form sulfate esters, which results in negatively charged cellulose nanocrystals (CNCs) that are electrostatically stable. The type of acid used determines the surface charge density of the CNCs, with sulfuric acid producing CNCs with higher surface charge density compared to hydrochloric acid. Therefore, different preparation routes can be employed to carry out various chemical modifications based on the desired properties of the CNCs. [100]. CNCs, as bio-based nanoscale materials, have captured the attention of both researchers in academia and industry due to their remarkable physicochemical and structural properties. These properties include high mechanical strength, optical transparency, tunable surface chemistry, low density, renewability, biodegradability, and biocompatibility [101]. As a result, CNCs are gaining recognition as a promising material for various applications in electronics [102], pharmaceuticals, biomedical, supercapacitors, membranes [103], and nanocomposites. Another type of nanocellulose is bacterial nanocellulose (BNCs), which is synthesized by different bacteria and has a very high degree of crystallinity [104]. Due to its hydrophilic surface chemistry, chemical inertness, high strength, and high surface area, NC has emerged as a promising material for water remediation applications [105]. While various approaches have been explored for water remediation, photocatalysis has gained attention due to its eco-friendly approach. Semiconductor materials have been investigated as photocatalysts; however, their agglomeration and limited reusability hinder their practical application [106]. Thus, the composites of these semiconductor materials with cellulose have been gaining attention due to their improved electron-hole pair separation. The cellulose materials provide structural support, immobilize the photocatalysts, and reduce their contamination, resulting in enhanced photocatalytic performance and recyclability [107]. To develop these composites, researchers have explored various semiconductor materials such as ZnO, TiO_2, WO^3, ZnS, CdS, BiOI, BiOBr, BiOCl, Ag_3PO_4, $AgVO_4$, AgI, AgBr, and $AgCrO_4$ [108].

Composites of semiconductors and cellulose have been found to improve photocatalytic activity by 1.3–3.5 times compared to individual semiconductors or cellulose. In recent times, non-metallic semiconductors such as carbon nitride and graphite have also been used to enhance photocatalysis [109]. This section will discuss the fundamental mechanism of photocatalysis and the use of cellulose-based photocatalysts for the degradation of organic pollutants in water and wastewater. Cellulose-based materials possess remarkable properties, including hy-

drophilicity, chirality, a large surface area, and versatile chemical functionality [110]. In particular, NC has been utilized as a photocatalyst for the degradation of organic pollutants in water under UV or visible light irradiation. Incorporating NPs with semiconductor properties has been shown to significantly increase the photocatalytic activity of NCs. Due to its exceptional host properties, cellulose can provide stability and effectively control the growth of NPs without compromising their morphology [111]. A great number of research has been conducted on the usage of nanocellulose (NC)-based materials, such as fibers, membranes, hybrid materials, and thin films, as photocatalysts for water remediation [112]. In hybrid materials consisting of cellulose and nanoparticles (NPs) such as TiO_2, ZnO, graphene oxide (GO), and Fe_2O_3, the cellulose is adsorbed onto the metal oxide, increasing the surface area and extending the wavelength response to the visible range through the incorporation of its hydroxyl (─OH) groups. Additionally, bacterial nanocellulose (BNC) has been employed for composite formation with metal oxide NPs because of its high surface-to-volume ratio, excellent hydrophilic properties, and remarkable mechanical strength [113]. Depending on the NPs used for hybrid formation, cellulose-based materials can be classified as follows:

4.4.1. TiO2/Nanocellulose composite as photocatalyst

Due to its high thermal stability, nontoxicity, cheap, and ease of handling, TiO_2 metal oxide is a semiconductor widely utilized for diverse applications such as photocatalysis and water splitting for hydrogen evolution reactions [114]. In this regard, Sun and colleagues developed a cellulose/TiO_2 composite monolith for the photocatalytic reduction of methylene blue (MB). Under UV light irradiation, the composite exhibited 99% removing within 60 minutes, and 90% efficiency retention after ten cycles [115]. In related research, a microfibrillated cellulose (MFC)-polyamide-amine-epichlorohydrin (PAE)-TiO_2 NP composite was developed using a two-step mixing process. The resulting composite was uniform, reproducible, flexible, and reusable. Under UV light irradiation, the composite demonstrated a 95% photocatalytic degradation of methyl orange within 150 minutes. The polyamide-amine played a essential role in retaining the NPs and preventing their release into the environment [111]. The photocatalytic reduction of MO in water has also been investigated using TiO_2 and bacterial nanocellulose (BNC). TiO_2 was supported onto the BNC, and rare earth elements were doped into the composite using the sol-gel method. The results demonstrated complete dye degradation using the (IV)-doped composite, while the (III)-doped composite exhibited 79.7% degradation. The optimal dosages for (IV) and (III) were 2 and 5 mol/L, respectively [30]. In addition, Brandes and colleagues synthesized spherical BC/TiO_2 nanocomposites for effective degradation of methylene blue from water. The nanocomposites demonstrated 70.83% and 89.58% degradation of MB after 35 minutes in situ and ex situ, respectively [116].

4.4.2. ZnO/Nanocellulose Composite as Photocatalyst

Cellulose nanocrystals (CNCs), which are prepared from natural cellulose via acid hydrolysis, are rod-shaped and can vary in size from 1 to 100 nm, depending mainly on their origin [117].

Chemical modifications and doping with other NPs, such as ZnO, have been used to alter the properties of cellulose nanocrystals (CNCs) for various applications in photocatalysis and the biomedical field. ZnO NPs have been found to possess high catalytic activity, optoelectronic properties, and disinfectant properties against a wide range of pathogens [28]. With a bandgap value of 3.3 eV, ZnO is a promising photocatalyst, similar to TiO_2 (which has a bandgap of 3.2 eV for anatase), and can be utilized for applications such as gas sensors, solar cells, UV photodetectors, optical devices, and batteries [118, 119]. Recent studies have also demonstrated the potential of ZnO NPs for wastewater treatment by degrading organic pollutants and other effluents [120, 121]. The use of ZnO as a photocatalyst is limited by its high surface energy and aggregation of nanoparticles, which can be overcome by incorporating nanofibrillar materials such as cellulose during their synthesis. Such nanocomposites have shown excellent applications in various fields, including wastewater treatment. Guan et al. developed hybrids of ZnO/CNC with varying morphologies using bamboo CNC as a precursor. The resulting hybrid exhibited high adsorption capacity for cationic dyes, with ZnO/CNC 8.5 showing efficient removal of malachite green (99.02%) and MB (93.55%) with an adsorption ability of 49.51 mg/g and 46.77 mg/g, respectively [122]. Researchers have also investigated the use of BNC as a photocatalyst for dye degradation. In addition, the composite of NC with ZnO has been developed using oil palm empty fruit bunches as a source of NC through alkaline and acid treatment, which acted as host polymers for the fabrication of ZnO NPs. The observed photocatalytic properties of ZnO/CN composite were found to be superior to those of pure ZnO, with the percentage crystalline index being improved from 35.7% to 43.3% and 53.3% by alkaline and acid treatment [123]. Furthermore, CNC/ZnO composites have demonstrated antibacterial activity and improved photocatalytic performance [124]. Researchers have also explored BNC as a potential photocatalyst for dye degradation [125]. Wei et al. utilized hydrothermal synthesis to develop hexagonal and crystalline wurtzite ZnO with BNC and used it for MB reduction in UV light irradiation. The photocatalyst showed 94.4% degradation efficiency within 30 minutes, and it was reusable for up to eight cycles. The use of cotton as a source of BNC makes it a renewable and eco-friendly material. The cellulose material acts as a substrate to immobilize the semiconductor NPs. In another study, Xiao et al. utilized TEMPO-oxidized cellulose as a reactive template to develop a carbon/ZnO composite for MB degradation, achieving up to 96.11% degradation within 120 minutes [126].

4.4.3. Graphene Oxide/Nanocellulose composite as photocatalyst

GO has been widely utilized for forming composites that improve the transmission capacity of e–/h+ pairs. The conjugate effect of the benzene ring in GO increases the photodegradation performance rate. Tu et al. produced a nanocomposite film of regenerated cellulose (RC) and GO with micropores incorporating Cu_2O NPs. The resulting nanocomposite was used for the reduction of MOdye invisible-light irradiation. The degradation rate increased from 2.0 mg/h/g/cat to 6.5 mg/h/g/cat [127]. Various solvents have been used as dispersing agents to enhance these films' electrical, thermal, and mechanical properties. The monohydrate solvent N-methylmorpholine-N-oxide (NMMO) was employed for fabricating GO/cellulose composite films, and their rheological properties were improved [128].

4.4.4. g-C3N4/Nanocellulose composite as photocatalyst

g-C3N4is a polymeric semiconductor that lacks metallic properties and has a bandgap of 2.7 eV, making it an ideal candidate for satisfying the thermodynamic requirements of water splitting to produce hydrogen and oxygen [129, 130]. Numerous research teams are currently exploring the capacity of g-C3N4 in the clean production of hydrogen [131]. While g-C3N4 shows superior photocatalytic performance for organic pollutant degradation compared to traditional photocatalysts such as TiO2, its composites with cellulose have demonstrated exceptional performance. In a study by Zhao et al., a composite membrane was synthesized using g-C3N4 nanosheet, rGO, and cellulose acetate (NS/rGO/CA), which was utilized for the reduction of rhodamine B dye in visible light irradiation. The observed photocatalytic performance was superior to that of g-C3N4 alone [109].

5. Conclusion and perspectives

The utilization of photocatalysis for water treatment is under visible light rapidly receiving popularity worldwide, and its distinct characteristics present significant opportunities to transform the field of water and wastewater treatment. This study gives a comprehensive overview of the recent advancements in photocatalytic water treatment, specifically focusing on photocatalysts under visible light irradiation. We delve into the fundamental principles of heterogeneous photocatalysis, the regulatory mechanism governing it, and the exceptional attributes of photocatalysts in visible light irradiation. Numerous techniques have been devised to expand the light absorption capability of photocatalysts to the visible spectrum, including doping, dye sensitization, heterostructure formation, incorporation of p-conjugated structures, and investigation of novel nanocomposites and multi-component oxides with visible light response. These modified photocatalysts have found extensive applications in degrading both organic and inorganic pollutants, as among with photocatalytic disinfection.

Hence, these findings hold potential for advancing the progress of environmentally friendly remediation techniques through redox reactions by photocatalyst propelled under visible light, a green energy source. Despite notable advancements in heterogeneous photocatalytic water treatment utilizing photocatalysts under visible light irradiation, this field remains in its early stages, and further improvements are necessary. While developing water treatment with photocatalysts poses important challenges, such as high costs, technical obstacles, and potential environmental and human hazards, many of these obstacles may be temporary in nature. In order to make photocatalytic water treatment technology in visible light irradiation a practical reality in the near term, it is crucial to address several critical technical challenges related to catalyst development, process optimization, and reactor design. These challenges include the need to enhance the efficiency and photo-stability photocatalysts, which are currently restricted by the physicochemical characteristics of these materials.

i) One modification technique, dye sensitization, has enabled the extension of adsorption light wavelength to the visible light range and enhanced the efficiency of conventional visible light responsive photocatalysts. However, the using of some photocatalytic materials remains restricted because of the degradation and dissolution issues associated with dyes, that hampers their photocatalytic applications. Thus, a more meticulous design of functional photocatalysts is necessary to achieve desirable physicochemical characteristic of the materials.

(ii) Creating a cost-effective solid-liquid separation method by effectively immobilising the photocatalyst. One significant challenge at present is the depletion of catalysts during the photocatalytic process, that impedes their regeneration and raises concerns about environmental contamination due to catalyst leakage. Immobilized photocatalytic systems can overcome issues related to catalyst recovery and aggregation, while also reducing the reactor's size.

(iii) Developing an efficient photoreactor to maximize the usage of solar energy and minimize electricity costs. The practical application of photocatalytic processes on an industrial scale necessitates the development of appropriate photoreactors. Proper design and construction of such devices can facilitate optimal harvesting of solar energy, efficient accommodation of photocatalysts and reactants, and effective collection of reaction products.

(iv) Developing a comprehensive global database containing information on the tested photocatalysts, including catalyst material types, preparation methods, improvement, photocatalytic reaction conditions, and performance. To prevent redundant and pointless efforts and to aid in the development of creative catalysts, this database should be easily accessible. Combining various techniques and approaches may be necessary to achieve the desired photo-degradation efficiency.

To this end, it is essential to establish a database containing comprehensive information on the construction and application of existing photocatalysts. Numerous nano materials have been utilized in photocatalysis under visible light irradiation, and creating a database will help in avoiding redundancy and accelerating progress. Additionally, theoretical and modeling studies should be conducted to develop a thorough understanding of the characteristics, synthesizing, and activity of photocatalysts and their modification for water treatment. Integrating multiple technologies can offer a promising outlook for water treatment and addressing energy concerns using advanced, highly efficient, and robust visible light-responsive photocatalysts.

REFERENCES

[1] H. Dai, X. Yuan, L. Jiang, H. Wang, J. Zhang, J. Zhang, T.J.C.C.R. Xiong, Recent advances on ZIF-8 composites for adsorption and photocatalytic wastewater pollutant removal: Fabrication, applications and perspective, 441 (2021) 213985.

[2] J. Qu, M.J.C.r.i.e.s. Fan, technology, The current state of water quality and technology development for water pollution control in China, 40(6) (2010) 519-560.

[3] D. Lapworth, N. Baran, M. Stuart, R.J.E.p. Ward, Emerging organic contaminants in groundwater: a review of sources, fate and occurrence, 163 (2012) 287-303.

[4] W. Liang, B. Wang, J. Cheng, D. Xiao, Z. Xie, J.J.J.o.H.M. Zhao, 3D, eco-friendly metal-organic frameworks@ carbon nanotube aerogels composite materials for removal of pesticides in water, 401 (2021) 123718.

[5] L. Joseph, B.-M. Jun, M. Jang, C.M. Park, J.C. Muñoz-Senmache, A.J. Hernández-Maldonado, A. Heyden, M. Yu, Y.J.C.E.J. Yoon, Removal of contaminants of emerging concern by metal-organic framework nanoadsorbents: A review, 369 (2019) 928-946.

[6] A.K. Verma, R.R. Dash, P.J.J.o.e.m. Bhunia, A review on chemical coagulation/flocculation technologies for removal of colour from textile wastewaters, 93(1) (2012) 154-168.

[7] N. Savage, M.S.J.J.o.N.r. Diallo, Nanomaterials and water purification: opportunities and challenges, 7 (2005) 331-342.

[8] G. Montes-Hernandez, N. Concha-Lozano, F. Renard, E.J.J.o.H.M. Quirico, Removal of oxyanions from synthetic wastewater via carbonation process of calcium hydroxide: Applied and fundamental aspects, 166(2-3) (2009) 788-795.

[9] Y.G. Solozhenko, N. Soboleva, V.J.J.o.W.C. Goncharuk, Technology, Physical Chemistry of Water Treatment Processes-Use of the H_2O_2-Fe^{2+} (Fe^{3+}) catalytic system in removing organic compounds from water, 26(3) (2004) 1-16.

[10] R.V. Prihod'ko, N.M.J.J.o.C. Soboleva, Photocatalysis: Oxidative processes in water treatment, 2013 (2013).

[11] M. Tanveer, G.T.J.R. Guyer, S.E. Reviews, Solar assisted photo degradation of wastewater by compound parabolic collectors: Review of design and operational parameters, 24 (2013) 534-543.

[12] L.-Y. Yang, S.-Y. Dong, J.-H. Sun, J.-L. Feng, Q.-H. Wu, S.-P.J.J.o.h.m. Sun, Microwave-assisted preparation, characterization and photocatalytic properties of a dumbbell-shaped ZnO photocatalyst, 179(1-3) (2010) 438-443.

[13] P. Fageria, S. Gangopadhyay, S.J.R.A. Pande, Synthesis of ZnO/Au and ZnO/Ag nanoparticles and their photocatalytic application using UV and visible light, 4(48) (2014) 24962-24972.

[14] S. Balachandran, S.G. Praveen, R. Velmurugan, M.J.R.A. Swaminathan, Facile fabrication of highly efficient, reusable heterostructured Ag–ZnO–CdO and its twin applications of dye degradation under natural sunlight and self-cleaning, 4(9) (2014) 4353-4362.

[15] S. Dong, J. Feng, M. Fan, Y. Pi, L. Hu, X. Han, M. Liu, J. Sun, J.J.R.A. Sun, Recent developments in heterogeneous photocatalytic water treatment using visible light-responsive photocatalysts: a review, 5(19) (2015) 14610-14630.

[16] Q. Zheng, H. Shen, D.J.E.S.W.R. Shuai, Technology, Emerging investigators series: advances and challenges of graphitic carbon nitride as a visible-light-responsive photocatalyst for sustainable water purification, 3(6) (2017) 982-1001.

[17] A. Kumar, P. Raizada, P. Singh, R.V. Saini, A.K. Saini, A.J.C.E.J. Hosseini-Bandegharaei, Perspective and status of polymeric graphitic carbon nitride based Z-scheme photocatalytic systems for sustainable photocatalytic water purification, 391 (2020) 123496.

[18] J.C. Colmenares, R.J.C.S.R. Luque, Heterogeneous photocatalytic nanomaterials: prospects and challenges in selective transformations of biomass-derived compounds, 43(3) (2014) 765-778.

[19] X. Li, R. Shen, S. Ma, X. Chen, J.J.A.S.S. Xie, Graphene-based heterojunction photocatalysts, 430 (2018) 53-107.

[20] Z. Zeng, Y.-B. Li, S. Chen, P. Chen, F.-X. Xiao, Insight into the charge transport correlation in Au_x clusters and graphene quantum dots deposited on TiO_2 nanotubes for photoelectrochemical oxygen evolution, (2018).
[21] P. Singh, B. Priya, P. Shandilya, P. Raizada, N. Singh, B. Pare, S.J.A.J.o.C. Jonnalagadda, Photocatalytic mineralization of antibiotics using 60% WO_3/BiOCl stacked to graphene sand composite and chitosan, 12(8) (2019) 4627-4645.
[22] V. Hasija, P. Raizada, A. Sudhaik, K. Sharma, A. Kumar, P. Singh, S.B. Jonnalagadda, V.K.J.A.M.T. Thakur, Recent advances in noble metal free doped graphitic carbon nitride based nanohybrids for photocatalysis of organic contaminants in water: a review, 15 (2019) 494-524.
[23] J. Yi, W. El-Alami, Y. Song, H. Li, P.M. Ajayan, H.J.C.E.J. Xu, Emerging surface strategies on graphitic carbon nitride for solar driven water splitting, 382 (2020) 122812.
[24] R.I.J.J.o.W.E. Harris, I. Aerodynamics, Discussion of "The annual rate of independent events for the analysis of extreme wind speed" by Alessio Torrielli, Maria Pia Repetto & Giovanni Solari, 100(164) (2017) 174-178.
[25] M. Chong, B. Jin, C. Chow, C.J.W.R. Saint, New developments in photocatalytic water treatment technology: a review, 44 (2010) 2997-3027.
[26] Y. Ma, X. Wang, Y. Jia, X. Chen, H. Han, C.J.C.r. Li, Titanium dioxide-based nanomaterials for photocatalytic fuel generations, 114(19) (2014) 9987-10043.
[27] C.J.A.C.A.G. Hariharan, Photocatalytic degradation of organic contaminants in water by ZnO nanoparticles: Revisited, 304 (2006) 55-61.
[28] K.M. Lee, C.W. Lai, K.S. Ngai, J.C.J.W.r. Juan, Recent developments of zinc oxide based photocatalyst in water treatment technology: a review, 88 (2016) 428-448.
[29] A. Kudo, Y.J.C.S.R. Miseki, Heterogeneous photocatalyst materials for water splitting, 38(1) (2009) 253-278.
[30] B. Donkova, D. Dimitrov, M. Kostadinov, E. Mitkova, D.J.M.C. Mehandjiev, Physics, Catalytic and photocatalytic activity of lightly doped catalysts M: ZnO (M= Cu, Mn), 123(2-3) (2010) 563-568.
[31] D. Zhang, F. Dai, P. Zhang, Z. An, Y. Zhao, L.J.M.S. Chen, E. C, The photodegradation of methylene blue in water with PVDF/GO/ZnO composite membrane, 96 (2019) 684-692.
[32] W.A. El-Yazeed, A.I.J.I.C.C. Ahmed, Photocatalytic activity of mesoporous WO3/TiO2 nanocomposites for the photodegradation of methylene blue, 105 (2019) 102-111.
[33] D. Matsunami, K. Yamanaka, T. Mizoguchi, K.J.J.o.P. Kojima, P.A. Chemistry, Comparison of photodegradation of methylene blue using various TiO_2 films and WO3 powders under ultraviolet and visible-light irradiation, 369 (2019) 106-114.
[34] M.M. Sabzehmeidani, H. Karimi, M.J.A.O.C. Ghaedi, Electrospinning preparation of NiO/ZnO composite nanofibers for photodegradation of binary mixture of rhodamine B and methylene blue in aqueous solution: central composite optimization, 32(6) (2018) e4335.
[35] P. Labhane, V. Huse, L. Patle, A. Chaudhari, G.J.J.o.M.S. Sonawane, C. Engineering, Synthesis of Cu doped ZnO nanoparticles: crystallographic, optical, FTIR, morphological and photocatalytic study, 3(07) (2015) 39.
[36] M. Fu, Y. Li, P. Lu, J. Liu, F.J.A.S.S. Dong, Sol–gel preparation and enhanced photocatalytic performance of Cu-doped ZnO nanoparticles, 258(4) (2011) 1587-1591.
[37] M. Thiruppathi, P.S. Kumar, P. Devendran, C. Ramalingan, M. Swaminathan, E.J.J.o.A. Nagarajan, Compounds, Ce@ TiO_2 nanocomposites: An efficient, stable and affordable photocatalyst for the photodegradation of diclofenac sodium, 735 (2018) 728-734.
[38] O. Nasr, O. Mohamed, A.-S. Al-Shirbini, A.-M.J.J.o.P. Abdel-Wahab, P.A. Chemistry, Photocatalytic degradation of acetaminophen over Ag, Au and Pt loaded TiO_2 using solar light, 374 (2019) 185-193.
[39] R. Zanella, E. Avella, R.M. Ramírez-Zamora, F. Castillón-Barraza, J.C.J.E.t. Durán-Álvarez, Enhanced photocatalytic degradation of sulfamethoxazole by deposition of Au, Ag and Cu metallic nanoparticles on TiO_2, 39(18) (2018) 2353-2364.
[40] Z.A.M. Hir, P. Moradihamedani, A.H. Abdullah, M.A.J.M.S.i.S.P. Mohamed, Immobilization of TiO_2 into polyethersulfone matrix as hybrid film photocatalyst for effective degradation of methyl orange dye, 57 (2017) 157-165.
[41] S. Das, S. Sinha, B. Das, R. Jayabalan, M. Suar, A. Mishra, A.J. Tamhankar, C. Stålsby Lundborg, S.K.J.S.r. Tripathy, Disinfection of multidrug resistant Escherichia coli by solar-photocatalysis using Fe-doped ZnO nanoparticles, 7(1) (2017) 104.
[42] C. Xu, L. Cao, G. Su, W. Liu, H. Liu, Y. Yu, X.J.J.o.h.m. Qu, Preparation of ZnO/Cu2O compound photocatalyst and application in treating organic dyes, 176(1-3) (2010) 807-813.
[43] C. Wang, B.-Q. Xu, X. Wang, J.J.J.o.S.S.C. Zhao, Preparation and photocatalytic activity of ZnO/TiO_2/SnO_2 mixture, 178(11) (2005) 3500-3506.
[44] R. Daghrir, P. Drogui, D.J.I. Robert, E.C. Research, Modified TiO_2 for environmental photocatalytic applications: a review, 52(10) (2013) 3581-3599.
[45] G. Cinelli, F. Cuomo, L. Ambrosone, M. Colella, A. Ceglie, F. Venditti, F.J.J.o.w.p.e. Lopez, Photocatalytic degradation of a model textile dye using Carbon-doped titanium dioxide and visible light, 20 (2017) 71-77.
[46] Y. Zhang, T. R Nayak, H. Hong, W.J.C.m.m. Cai, Biomedical applications of zinc oxide nanomaterials, 13(10) (2013) 1633-1645.
[47] K. Milenova, I. Stambolova, V. Blaskov, A. Eliyas, S. Vassilev, M.J.J.o.c.t. Shipochka, metallurgy, The effect of introducing copper dopant on the photocatalytic activity of ZnO nanoparticles, 48(3) (2013) 259-264.
[48] E. Sharmin, F. Zafar, Introductory chapter: metal organic frameworks (MOFs), Metal-organic frameworks, IntechOpen2016.
[49] M. Alhamami, H. Doan, C.-H.J.M. Cheng, A review on breathing behaviors of metal-organic-frameworks (MOFs) for gas adsorption, 7(4) (2014) 3198-3250.
[50] J.D. Evans, B. Garai, H. Reinsch, W. Li, S. Dissegna, V. Bon, I. Senkovska, R.A. Fischer, S. Kaskel, C.J.C.C.R. Janiak, Metal–organic frameworks in Germany: From synthesis to function, 380 (2019) 378-418.
[51] J.-D. Xiao, H.-L.J.A.o.C.R. Jiang, Metal–organic frameworks for photocatalysis and photothermal catalysis, 52(2) (2018) 356-366.
[52] H. Furukawa, K.E. Cordova, M. O'Keeffe, O.M.J.S. Yaghi, The chemistry and applications of metal-organic frameworks, 341(6149) (2013) 1230444.
[53] A. Kirchon, L. Feng, H.F. Drake, E.A. Joseph, H.-C.J.C.S.R. Zhou, From fundamentals to applications: a toolbox for robust and multifunctional MOF materials, 47(23) (2018) 8611-8638.
[54] D.J. Tranchemontagne, K.S. Park, H. Furukawa, J. Eckert, C.B. Knobler, O.M.J.T.J.o.P.C.C. Yaghi, Hydrogen storage in new metal–organic frameworks, 116(24) (2012) 13143-13151.
[55] C. Zhang, L. Ai, J.J.J.o.M.C.A. Jiang, Solvothermal synthesis of MIL–53 (Fe) hybrid magnetic composites for photoelectrochemical water oxidation and organic pollutant photodegradation under visible light, 3(6) (2015) 3074-3081.
[56] J.-J. Du, Y.-P. Yuan, J.-X. Sun, F.-M. Peng, X. Jiang, L.-G. Qiu, A.-J. Xie, Y.-H. Shen, J.-F.J.J.o.h.m. Zhu, New photocatalysts based on MIL-53 metal–organic frameworks for the decolorization of methylene blue dye, 190(1-3) (2011) 945-951.
[57] J. Gascon, M.D. Hernández-Alonso, A.R. Almeida, G.P. van Klink, F. Kapteijn, G.J.C.C. Mul, S. Energy, Materials, Isoreticular MOFs as efficient photocatalysts with tunable band gap: an operando FTIR study of the photoinduced oxidation of propylene, 1(12) (2008) 981-983.
[58] L. Zeng, X. Guo, C. He, C.J.A.C. Duan, Metal–organic frameworks: versatile materials for heterogeneous photocatalysis, 6(11) (2016) 7935-7947.
[59] V.K. Sharma, M.J.J.o.h.m. Feng, Water depollution using metal-organic frameworks-catalyzed advanced oxidation processes: a review, 372 (2019) 3-16.
[60] K.J.C. Sing, S.A. Physicochemical, E. Aspects, The use of nitrogen adsorption for the characterisation of porous materials, 187 (2001) 3-9.
[61] M. Alvaro, E. Carbonell, B. Ferrer, F.X. Llabrés i Xamena, H.J.C.A.E.J. Garcia, Semiconductor behavior of a metal-organic framework (MOF), 13(18) (2007) 5106-5112.
[62] S. Hausdorf, J.r. Wagler, R. Moβig, F.O.J.T.J.o.P.C.A. Mertens, Proton and water activity-controlled structure formation in zinc carboxylate-based metal organic frameworks, 112(33) (2008) 7567-7576.
[63] K.G. Laurier, F. Vermoortele, R. Ameloot, D.E. De Vos, J. Hofkens, M.B.J.J.o.t.A.C.S. Roeffaers, Iron (III)-based metal–organic frameworks as visible light photocatalysts, 135(39) (2013) 14488-14491.
[64] L. Shi, T. Wang, H. Zhang, K. Chang, X. Meng, H. Liu, J.J.A.s. Ye, An amine-functionalized iron (III) metal–organic framework as efficient visible-light photocatalyst for Cr (VI) reduction, 2(3) (2015) 1500006.
[65] S. Mosleh, M.R.J.U.S. Rahimi, Intensification of abamectin pesticide degradation using the combination of ultrasonic cavitation and visible-light driven photocatalytic process: synergistic effect and optimization study, 35 (2017) 449-457.
[66] A.K. Geim, K.S.J.N.m. Novoselov, The rise of graphene, 6(3) (2007) 183-191.
[67] A.S. Mayorov, R.V. Gorbachev, S.V. Morozov, L. Britnell, R. Jalil, L.A. Ponomarenko, P. Blake, K.S. Novoselov, K. Watanabe, T.J.N.l. Taniguchi, Micrometer-scale ballistic transport in encapsulated graphene at room temperature, 11(6) (2011) 2396-2399.
[68] J.-U. Lee, D. Yoon, H.J.N.l. Cheong, Estimation of Young's modulus of graphene by Raman spectroscopy, 12(9) (2012) 4444-4448.
[69] M.D. Stoller, S. Park, Y. Zhu, J. An, R.S.J.N.l. Ruoff, Graphene-based ultracapacitors, 8(10) (2008) 3498-3502.
[70] X. Li, Y. Zhu, W. Cai, M. Borysiak, B. Han, D. Chen, R.D. Piner, L. Colombo, R.S.J.N.l. Ruoff, Transfer of large-area graphene films for high-performance transparent conductive electrodes, 9(12) (2009) 4359-4363.

[71] S. Chen, Q. Wu, C. Mishra, J. Kang, H. Zhang, K. Cho, W. Cai, A.A. Balandin, R.S.J.N.m. Ruoff, Thermal conductivity of isotopically modified graphene, 11(3) (2012) 203-207.
[72] J. Moser, A. Barreiro, A.J.A.P.L. Bachtold, Current-induced cleaning of graphene, 91(16) (2007) 163513.
[73] X. Wang, L. Zhi, K.J.N.l. Müllen, Transparent, conductive graphene electrodes for dye-sensitized solar cells, 8(1) (2008) 323-327.
[74] P. Blake, P.D. Brimicombe, R.R. Nair, T.J. Booth, D. Jiang, F. Schedin, L.A. Ponomarenko, S.V. Morozov, H.F. Gleeson, E.W.J.N.l. Hill, Graphene-based liquid crystal device, 8(6) (2008) 1704-1708.
[75] M.F. El-Kady, V. Strong, S. Dubin, R.B.J.S. Kaner, Laser scribing of high-performance and flexible graphene-based electrochemical capacitors, 335(6074) (2012) 1326-1330.
[76] K.C. Kemp, H. Seema, M. Saleh, N.H. Le, K. Mahesh, V. Chandra, K.S.J.N. Kim, Environmental applications using graphene composites: water remediation and gas adsorption, 5(8) (2013) 3149-3171.
[77] O. Akhavan, E.J.A.n. Ghaderi, Toxicity of graphene and graphene oxide nanowalls against bacteria, 4(10) (2010) 5731-5736.
[78] R.K. Upadhyay, N. Soin, S.S.J.R.a. Roy, Role of graphene/metal oxide composites as photocatalysts, adsorbents and disinfectants in water treatment: a review, 4(8) (2014) 3823-3851.
[79] D.Y. Lyon, L. Brunet, G.W. Hinkal, M.R. Wiesner, P.J.J.N.l. Alvarez, Antibacterial activity of fullerene water suspensions (nC60) is not due to ROS-mediated damage, 8(5) (2008) 1539-1543.
[80] C.D. Vecitis, K.R. Zodrow, S. Kang, M.J.A.n. Elimelech, Electronic-structure-dependent bacterial cytotoxicity of single-walled carbon nanotubes, 4(9) (2010) 5471-5479.
[81] Y. Yang, L. Ren, C. Zhang, S. Huang, T.J.A.a.m. Liu, interfaces, Facile fabrication of functionalized graphene sheets (FGS)/ZnO nanocomposites with photocatalytic property, 3(7) (2011) 2779-2785.
[82] S. Liu, M. Hu, T.H. Zeng, R. Wu, R. Jiang, J. Wei, L. Wang, J. Kong, Y.J.L. Chen, Lateral dimension-dependent antibacterial activity of graphene oxide sheets, 28(33) (2012) 12364-12372.
[83] E. Valsami-Jones, I.J.S. Lynch, How safe are nanomaterials?, 350(6259) (2015) 388-389.
[84] Z. Wang, B.J.E.s. Mi, technology, Environmental applications of 2D molybdenum disulfide (MoS2) nanosheets, 51(15) (2017) 8229-8244.
[85] G. Li, X. Nie, J. Chen, Q. Jiang, T. An, P.K. Wong, H. Zhang, H. Zhao, H.J.W.r. Yamashita, Enhanced visible-light-driven photocatalytic inactivation of Escherichia coli using g-C_3N_4/TiO_2 hybrid photocatalyst synthesized using a hydrothermal-calcination approach, 86 (2015) 17-24.
[86] J. Bai, Z. Wang, P. Zhou, P. Xu, Y. Deng, Q.J.A.S.S. Zhou, Rapid thermal surface engineering of g-C_3N_4 for efficient hydrogen evolution, 539 (2021) 148308.
[87] R.L.J.A.n. Whitby, Chemical control of graphene architecture: tailoring shape and properties, 8(10) (2014) 9733-9754.
[88] L. Liao, H. Peng, Z.J.J.o.t.A.c.s. Liu, Chemistry makes graphene beyond graphene, 136(35) (2014) 12194-12200.
[89] V. Georgakilas, J.A. Perman, J. Tucek, R.J.C.r. Zboril, Broad family of carbon nanoallotropes: classification, chemistry, and applications of fullerenes, carbon dots, nanotubes, graphene, nanodiamonds, and combined superstructures, 115(11) (2015) 4744-4822.
[90] P. Fernandez-Ibanez, M. Polo-López, S. Malato, S. Wadhwa, J. Hamilton, P. Dunlop, R. D'sa, E. Magee, K. O'shea, D.J.C.E.J. Dionysiou, Solar photocatalytic disinfection of water using titanium dioxide graphene composites, 261 (2015) 36-44.
[91] Y. Pang, Y. Li, G. Xu, Y. Hu, Z. Kou, Q. Feng, J. Lv, Y. Zhang, J. Wang, Y.J.A.C.B.E. Wu, Z-scheme carbon-bridged Bi_2O_3/TiO_2 nanotube arrays to boost photoelectrochemical detection performance, 248 (2019) 255-263.
[92] O. Akhavan, M. Abdolahad, Y. Abdi, S.J.C. Mohajerzadeh, Synthesis of titania/carbon nanotube heterojunction arrays for photoinactivation of E. coli in visible light irradiation, 47(14) (2009) 3280-3287.
[93] O. Akhavan, R. Azimirad, S. Safa, M.J.J.o.M.C. Larijani, Visible light photo-induced antibacterial activity of CNT–doped TiO_2 thin films with various CNT contents, 20(35) (2010) 7386-7392.
[94] J. Zhang, X. Liu, X. Wang, L. Mu, M. Yuan, B. Liu, H.J.J.o.h.m. Shi, Carbon dots-decorated $Na_2W_4O_{13}$ composite with WO_3 for highly efficient photocatalytic antibacterial activity, 359 (2018) 1-8.
[95] X. Zeng, S. Lan, I.M.J.E.S.N. Lo, Rapid disinfection of E. coli by a ternary BiVO 4/Ag/gC 3 N 4 composite under visible light: photocatalytic mechanism and performance investigation in authentic sewage, 6(2) (2019) 610-623.
[96] A.J.C.O.i.C. Dufresne, I. Science, Cellulose nanomaterial reinforced polymer nanocomposites, 29 (2017) 1-8.
[97] S.J.C.p. Mondal, Preparation, properties and applications of nanocellulosic materials, 163 (2017) 301-316.
[98] H. Xie, H. Du, X. Yang, C.J.I.J.o.P.S. Si, Recent strategies in preparation of cellulose nanocrystals and cellulose nanofibrils derived from raw cellulose materials, 2018 (2018).
[99] A. Isogai, Y.J.C.O.i.S.S. Zhou, M. Science, Diverse nanocelluloses prepared from TEMPO-oxidized wood cellulose fibers: Nanonetworks, nanofibers, and nanocrystals, 23(2) (2019) 101-106.
[100] F. Niu, M. Li, Q. Huang, X. Zhang, W. Pan, J. Yang, J.J.C.P. Li, The characteristic and dispersion stability of nanocellulose produced by mixed acid hydrolysis and ultrasonic assistance, 165 (2017) 197-204.
[101] Y.-Y. Li, B. Wang, M.-G. Ma, B.J.I.J.o.P.S. Wang, Review of recent development on preparation, properties, and applications of cellulose-based functional materials, 2018 (2018).
[102] C. Chen, L.J.A.o.c.r. Hu, Nanocellulose toward advanced energy storage devices: structure and electrochemistry, 51(12) (2018) 3154-3165.
[103] H. Voisin, L. Bergström, P. Liu, A.P.J.N. Mathew, Nanocellulose-based materials for water purification, 7(3) (2017) 57.
[104] P.C. Faria-Tischer, R.M. Ribeiro-Viana, C.A. Tischer, Bio-based nanocom -posites: Strategies for cellulose functionalization and tissue affinity studies, Mate -rials for biomedical engineering, Elsevier2019, pp. 205-244.
[105] C. Jiménez Saelices, I.J.B. Capron, Design of Pickering micro-and nanoemulsions based on the structural characteristics of nanocelluloses, 19(2) (2018) 460-469.
[106] S.-Y. Lee, S.-J.J.J.o.i. Park, e. chemistry, TiO_2 photocatalyst for water treatment applications, 19(6) (2013) 1761-1769.
[107] K. Kim, P.G. Ingole, S. Yun, W. Choi, J. Kim, H.J.J.o.C.T. Lee, Water vapor removal using CA/PEG blending materials coated hollow fiber membrane, Biotechnology, 90(6) (2015) 1117-1123.
[108] Y. Zhao, Y. Wang, G. Xiao, H.J.C.J.o.C.E. Su, Fabrication of biomaterial/TiO2 composite photocatalysts for the selective removal of trace environmental pollutants, 27(6) (2019) 1416-1428.
[109] H. Zhao, S. Chen, X. Quan, H. Yu, H.J.A.C.B.E. Zhao, Integration of microfiltration and visible-light-driven photocatalysis on g-C_3N_4 nanosheet/reduced graphene oxide membrane for enhanced water treatment, 194 (2016) 134-140.
[110] S.H. Osong, S. Norgren, P.J.C. Engstrand, Processing of wood-based microfibrillated cellulose and nanofibrillated cellulose, and applications relating to papermaking: a review, 23 (2016) 93-123.
[111] U.M. Garusinghe, V.S. Raghuwanshi, W. Batchelor, G.J.S.r. Garnier, Water resistant cellulose–titanium dioxide composites for photocatalysis, 8(1) (2018) 2306.
[112] Y. Nevo, N. Peer, S. Yochelis, M. Igbaria, S. Meirovitch, O. Shoseyov, Y.J.R.A. Paltiel, Nano bio optically tunable composite nanocrystalline cellulose films, 5(10) (2015) 7713-7719.
[113] M. Xu, H. Wang, G. Wang, L. Zhang, G. Liu, Z. Zeng, T. Ren, W. Zhao, X. Wu, Q.J.J.o.M.S. Xue, Study of synergistic effect of cellulose on the enhancement of photocatalytic activity of ZnO, 52 (2017) 8472-8484.
[114] A. Wittmar, H. Thierfeld, S. Köcher, M.J.R.A. Ulbricht, Routes towards cata -lytically active TiO_2 doped porous cellulose, 5(45) (2015) 35866-35873.
[115] X. Sun, K. Wang, Y. Shu, F. Zou, B. Zhang, G. Sun, H. Uyama, X.J.M. Wang, One-pot route towards active TiO_2 doped hierarchically porous cellulose: highly efficient photocatalysts for methylene blue degradation, 10(4) (2017) 373.
[116] R. Brandes, E.C. Trindade, D.F. Vanin, V.M. Vargas, C.A. Carminatti, H.A. Al-Qureshi, D.O.J.F. Recouvreux, Polymers, Spherical bacterial cellulose/TiO_2 nanocomposite with potential application in contaminants removal from wastewater by photocatalysis, 19 (2018) 1861-1868.
[117] D. Trache, M.H. Hussin, M.M. Haafiz, V.K.J.N. Thakur, Recent progress in cellulose nanocrystals: sources and production, 9(5) (2017) 1763-1786.
[118] S. Singh, R. Pendurthi, M. Khanuja, S. Islam, S. Rajput, S.J.A.P.A. Shivaprasad, Copper-doped modified ZnO nanorods to tailor its light assisted charge transfer reactions exploited for photo-electrochemical and photo-catalytic application in environmental remediation, 123 (2017) 1-10.
[119] F. Awan, M.S. Islam, Y. Ma, C. Yang, Z. Shi, R.M. Berry, K.C.J.A.o. Tam, Cellulose nanocrystal–ZnO nanohybrids for controlling photocatalytic activity and UV protection in cosmetic formulation, 3(10) (2018) 12403-12411.
[120] M. Samadi, M. Zirak, A. Naseri, E. Khorashadizade, A.Z.J.T.S.F. Moshfegh ,Recent progress on doped ZnO nanostructures for visible-light photocatalysis, 605(2016) 2-19.
[121] P.R. Sharma, S.K. Sharma, R. Antoine, B.S.J.A.S.C. Hsiao, Engineering, Efficient removal of arsenic using zinc oxide nanocrystal-decorated regenerated microfibrillated cellulose scaffolds, 7(6) (2019) 6140-6151.
[122] Y. Guan, H.-Y. Yu, S.Y.H. Abdalkarim, C. Wang, F. Tang, J. Marek, W.-L.

Chen, J. Militky, J.-M.J.I.j.o.b.m. Yao, Green one-step synthesis of ZnO/cellulose nanocrystal hybrids with modulated morphologies and superfast absorption of cationic dyes, 132 (2019) 51-62.
[123] K. Lefatshe, C.M. Muiva, L.P.J.C.p. Kebaabetswe, Extraction of nanocellulose and in-situ casting of ZnO/cellulose nanocomposite with enhanced photocatalytic and antibacterial activity, 164 (2017) 301-308.
[124] H.-Y. Yu, G.-Y. Chen, Y.-B. Wang, J.-M.J.C. Yao, A facile one-pot route for preparing cellulose nanocrystal/zinc oxide nanohybrids with high antibacterial and photocatalytic activity, 22 (2015) 261-273.
[125] W.-l. Zheng, W.-l. Hu, S.-y. Chen, Y. Zheng, B.-h. Zhou, H.-p.J.C.J.o.P.S. Wang, High photocatalytic properties of zinc oxide nanoparticles with amidoximated bacterial cellulose nanofibers as templates, 32(2) (2014) 169-176.
[126] H. Xiao, W. Zhang, Y. Wei, L.J.C. Chen, Carbon/ZnO nanorods composites templated by TEMPO-oxidized cellulose and photocatalytic activity for dye degradation, 25 (2018) 1809-1819.
[127] K. Tu, Q. Wang, A. Lu, L.J.T.J.o.P.C.C. Zhang, Portable visible-light photocatalysts constructed from Cu_2O nanoparticles and graphene oxide in cellulose matrix, 118(13) (2014) 7202-7210.
[128] C.-J. Kim, W. Khan, D.-H. Kim, K.-S. Cho, S.-Y.J.C.p. Park, Graphene oxide/cellulose composite using NMMO monohydrate, 86(2) (2011) 903-909.
[129] F. Su, S.C. Mathew, G. Lipner, X. Fu, M. Antonietti, S. Blechert, X.J.J.o.t.A.C.S. Wang, mpg-C_3N_4-catalyzed selective oxidation of alcohols using O2 and visible light, 132(46) (2010) 16299-16301.
[130] M. Bellardita, E.I. García-López, G. Marcì, I. Krivtsov, J.R. García, L.J.A.C.B.E. Palmisano, Selective photocatalytic oxidation of aromatic alcohols in water by using P-doped g-C_3N_4, 220 (2018) 222-233.
[131] X. Wang, K. Maeda, A. Thomas, K. Takanabe, G. Xin, J.M. Carlsson, K. Domen, M.J.N.m. Antonietti, A metal-free polymeric photocatalyst for hydrogen production from water under visible light, 8(1) (2009) 76-80.
[132] H. Karimi-Maleh, B.G. Kumar, S. Rajendran, J. Qin, S. Vadivel, D. Durgalakshmi, F. Gracia, M. Soto-Moscoso, Y. Orooji, F.J.J.o.M.L. Karimi, Tuning of metal oxides photocatalytic performance using Ag nanoparticles integration, 314 (2020) 113588.
[133] Y.N. Rajeev, C.M. Magdalane, G. Ramalingam, L.B. Kumar, N. Alwadai, M.J.A.P.A. Al-Buriahi, Photocatalytic activity of hierarchical CTAB-assisted TiO_2 nanoparticles for polluted water treatment using solar light illumination, 128(4) (2022) 299.
[134] S.E. Mousavi, H. Younesi, N. Bahramifar, P. Tamunaidu, H.J.C. Karimi-Maleh, A novel route to the synthesis of α-Fe_2O_3@ C@ SiO_2/TiO_2 nanocomposite from the metal-organic framework as a photocatalyst for water treatment, 297 (2022) 133992.
[135] M.L. Matias, A. Pimentel, A.S. Reis-Machado, J. Rodrigues, J. Deuermeier, E. Fortunato, R. Martins, D.J.N. Nunes, Enhanced Fe-TiO_2 Solar Photocatalysts on Porous Platforms for Water Purification, 12(6) (2022) 1005.
[136] Z. Kong, L. Lu, C. Zhu, J. Xu, Q. Fang, R. Liu, Y.J.S. Shen, P. Technology, Enhanced adsorption and photocatalytic removal of PFOA from water by F-functionalized MOF with in-situ-growth TiO_2: Regulation of electron density and band-gap, 297 (2022) 121449.
[137] Y. Zhou, L. Zhou, C. Ni, E. He, L. Yu, X.J.J.o.A. Li, Compounds, 3D/2D MOF-derived CoCeOx/g-C_3N_4 Z-scheme heterojunction for visible light photocatalysis: Hydrogen production and degradation of carbamazepine, 890 (2022) 161786.
[138] J. Xue, M. Xu, J. Gao, Y. Zong, M. Wang, S.J.C. Ma, S.A. Physicochemical, E. Aspects, Multifunctional porphyrinic Zr-MOF composite membrane for high-performance oil-in-water separation and organic dye adsorption/photocatalysis, 628 (2021) 127288.
[139] J.-L. Qiu, J. Su, N. Muhammad, W.-T. Zheng, C.-L. Yue, F.-Q. Liu, J.-L. Zuo, Z.-J.J.C.E.J. Ding, Facile encapsulating Ag nanoparticles into a tetrathiafulvalene-based Zr-MOF for enhanced photocatalysis, 427 (2022) 131970.
[140] R.R. Solís, M. Peñas-Garzón, C. Belver, J.J. Rodriguez, J.J.J.o.E.C.E. Bedia, Highly stable UiO-66-NH2 by the microwave-assisted synthesis for solar photocatalytic water treatment, 10(2) (2022) 107122.
[141] Y. Shi, D. Wan, J. Huang, Y. Liu, J.J.C. Li, Stable LBL self-assembly coating porous membrane with 3D heterostructure for enhanced water treatment under visible light irradiation, 252 (2020) 126581.
[142] S. Hmamouchi, A. El Yacoubi, A. Massit, M. Berradi, M. El Hezzat, B. Sallek, B.C.J.M.T.P. El Idrissi, Photocatalytic decomposition of methylene blue dye using sand-graphite composite under visible light irradiation, 72 (2023) 3677-3685.
[143] H. Ming, D. Wei, Y. Yang, B. Chen, C. Yang, J. Zhang, Y.J.C.E.J. Hou, Photocatalytic activation of peroxymonosulfate by carbon quantum dots functionalized carbon nitride for efficient degradation of bisphenol A under visible-light irradiation, 424 (2021) 130296.
[144] L. Lebogang, R. Bosigo, K. Lefatshe, C.J.M.C. Muiva, Physics, Ag_3PO_4/nanocellulose composite for effective sunlight driven photodegradation of organic dyes in wastewater, 236 (2019) 121756.
[145] M.S. Vasheghani Farahani, M. Nikzad, M.J.C. Ghorbani, Fabrication of fe-doped ZnO/nanocellulose nanocomposite as an efficient photocatalyst for degradation of methylene blue under visible light, 29(13) (2022) 7277-7299.
[146] G.-q. Liu, X.-j. Pan, J. Li, C. Li, C.-l.J.J.o.S.C.S. Ji, Facile preparation and characterization of anatase TiO_2/nanocellulose composite for photocatalytic degradation of methyl orange, 25(12) (2021) 101383.
[147] J. Nahi, A. Radhakrishnan, B.J.M.T.P. Beena, Green synthesis of zinc oxide incorporated nanocellulose with visible light photocatalytic activity and application for the removal of antibiotic enrofloxacin from aqueousmedia, 41 (2021) 583-589.
[148] R.G. Toro, A.M. Adel, T. de Caro, B. Brunetti, M.T. Al-Shemy, D.J.M. Caschera, A Facile One-Pot Approach to the Fabrication of Nanocellulose–Titanium Dioxide Nanocomposites with Promising Photocatalytic and Antimicrobial Activity, 15(16) (2022) 5789.